# Low Surface Energy Polystyrene

**Jens Höpken and Martin Möller***

*Department of Chemical Technology, University of Twente, P.O. Box 217, 7500 AE Enschede, The Netherlands*

*Received July 17, 1991*

ABSTRACT: Styrene monomers carrying $C_4F_9$ and $C_8H_{17}$ fluorocarbon substituents have been prepared by phase-transfer-catalyzed etherification of alcohols with perfluorinated segments and *p*-(chloromethyl)styrene. Homopolymers as well as copolymers with different molar amounts of styrene as the second comonomer were prepared by radical initiation. Thermal characterization demonstrated a decrease of the glass transition with an increase in the fraction of fluorocarbon substituents. Side-chain crystallization was observed for the homopolymer containing perfluorooctyl segments. For this polymer, a remarkably low critical surface tension was found by dynamic contact angle measurements, indicating the formation of a highly ordered layer of fluorocarbon segments at the polymer surface. Polymers containing small amounts of fluorinated comonomer units still had considerably reduced surface energies compared to pure polystyrene. Preferential adsorption and organization of fluorinated segments at the material surface were more pronounced with longer fluorocarbon moieties.

## Introduction

Polymers with highly fluorinated side chains have found a number of applications based on properties which are a consequence of the low surface energy of these materials. Fluorine-containing polymers are generally resistent against organic solvents and aggressive chemicals.[1] Copolymers with small amounts of fluorinated comonomers improve the water-repellant characteristics of the material.[2] Due to their low friction coefficient, viscous fluorinated oligomers are employed as efficient lubricants.[3] The surface properties which lead to these applications result from the incompatibility of short perfluorinated segments with hydrocarbons as well as with water and other polar components.

The extent of the lowering of the polymer surface energy depends not only on the coverage of the surface by fluorocarbon segments but also on the degree of ordering in the surface layer. The work of Zisman[4] demonstrated that the surface of lowest energy, the surface that provides best protection, is made up of an ideal close-packed array of trifluoromethyl groups. This ideal situation has been successfully approached by the adsorption of fluorocarbon chain molecules with reactive end groups on highly polar metal or metal oxide surfaces.[5] A second method is the Langmuir–Blodgett deposition of monolayers of ionic fluorocarbon surfactants on solid substrates. While nonionic surfactants gave a partially ordered, tilted arrangement of the fluorocarbon segments at the surface,[6,7] the presence of ionic head groups facilitated the ordering of the fluorocarbon segments.[8]

Studies on nonpolar low molecular weight hydrocarbon molecules which contain a perfluorinated segment demonstrated that their behavior and their properties are dominated by the peculiar incompatibility of the two segments.[9] Fluorocarbon–hydrocarbon diblock molecules, $F(CF_2)_n(CH_2)_mR$ (R = H, $OCH_2CH{=}CH_2$, $OOC(CH_3){-}C{=}CH_2$), crystallize in bilayer lamellar structures.[10,11] Most of the compounds show at least two disordering transitions before isotropization.[9,12,13] The disordered mesophases show smectic liquid-crystalline layer structures.[14,15] In organic solution, the fluorocarbon–hydrocarbon molecules get preferentially adsorbed at the solution/air interface and cause a steep decrease of the surface tension at low concentrations, which is similar to the behavior of surfactant solutions with a critical micelle concentration.[12,13] Generally, also an aggregation of the diblock molecules is found in fluorocarbon solution.[16] In a special case, the existence of micellelike associates was observed also in hydrocarbon solvents.[9] Crystallization from organic solvents resulted in the formation of needle crystals which become interlocked in disarray and form a three-dimensional network, which encloses the solvent in the cavities.[9] All these results demonstrate that low molecular weight semifluorinated molecules associate to self-organized supermolecular structures in the bulk as well as in hydrocarbon solution.

The work reported here is aimed at the preparation of high molecular weight materials containing fluorocarbon segments which can organize to defined supramolecular structures such as monomolecular surface layers. Such amphiphilic polymers are interesting as compatibilizers for blends of hydrocarbon polymers with fluorocarbon polymers, and their association behavior and surface activity direct interest toward the development of additives for polymer melts and the modification of polymer surface properties. Thus, materials with ordered fluorocarbon surfaces of extremely low surface energy can be prepared.

## Experimental Part

**Materials:** Styrene (Merck; 99%) was distilled under reduced pressure (50 mmHg), first from potassium hydroxide and then from calcium hydride, and stored under argon. 2,2′-Azobis(isobutyronitrile) (97%; Merck) was recrystallized from methanol below 40 °C. *p*-(Chloromethyl)styrene (Nagase & Co. Ltd., Tokyo, Japan), 1*H*,1*H*,2*H*,2*H*-perfluoroalkanols (98%; Hoechst AG), tetrabutylammonium hydrogen sulfate (TBAH, 97%; Merck), and solvents (Merck p.a.) were used without further purification.

***p*-Perfluoroalkyl-ethyleneoxymethyl styrenes:** 1*H*,1*H*,2*H*,2*H*-Perfluorohexanol or 1*H*,1*H*,2*H*,2*H*-perfluorodecanol (80 mmol) was mixed with 160 mL of 50% aqueous NaOH. Amounts of 160 mL of methylene chloride and 8 mmol of TBAH were added, and the resulting suspension was vigorously stirred. Upon addition of 88 mmol *p*-(chloromethyl)styrene, the reaction mixture turned brilliant yellow. After stirring for 18 h at 40 °C, the orange organic layer was separated, washed once with dilute hydrochloric acid and three times with water, and dried over sodium sulfate. Brown oily liquids were obtained after filtration and evaporation of the solvent. The monomer with a $C_4$ fluorocarbon segment was purified by distillation in high vacuum, giving a colorless, oily liquid. The compound with a $C_8$ fluorocarbon segment was repeatedly recrystallized from methanol, yielding white waxy crystals.

* To whom all correspondence should be addressed.

0024-9297/92/2225-1461$03.00/0 

$F(CF_2)_4CH_2CH_2OCH_2C_6H_4CH{=}CH_2$: yield = 76%, purity = 97% (GC), bp = 75 °C ($10^{-2}$ mmHg), mp = −23 °C (DSC). $^1H$ NMR ($CDCl_3$): $\delta_{TMS}$ 2.45 (2 protons, $CF_2CH_2$, tripled triplet, $J_{H-F}$ = 18 Hz, $J_{H-H}$ = 6 Hz), 3.77 (2 protons, $CF_2CH_2CH_2O$, t), 4.54 (2 protons, $OCH_2C_6H_4$, s), 5.26 (1 proton, trans HCH=C-$HC_6H_4$, d, $J$ = 12 Hz), 5.76 (1 proton, cis HCH=$CHC_6H_4$, d, $J$ = 18 Hz), 6.73 (1 proton, $CH_2{=}CHC_6H_4$, q), 7.36 (4 aromatic protons, two doublets).

$F(CF_2)_8CH_2CH_2OCH_2C_6H_4CH{=}CH_2$: yield = 82%, purity = 97% (GC), disordering transition = 11 °C, mp = 32 °C (DSC). $^1H$ NMR: see spectrum for $F(CF_2)_4CH_2CH_2OCH_2C_6H_4CH{=}CH_2$ given above.

**Radical polymerization**: [[(perfluoroalkylethylene)oxy]methyl]styrenes and styrene were used as (co)monomers for the preparation of fluorocarbon-containing polymers. Monomers were filled into flasks together with 5 mol % of AIBN and 30 wt % of toluene; the solutions were degassed by two freeze–pump–thaw cycles and heated first to 60 °C for 14 h and then to 90 °C for another 4 h. The viscous solutions were diluted with 4 times the amount of toluene, and the polymers were precipitated into methanol. The homopolymer prepared from $F(CF_2)_8(CH_2)_2OCH_2C_6H_4CH{=}CH_2$ was not sufficiently soluble in toluene and therefore dissolved in trichlorotrifluoroethane (F113). Polymers were purified by repeated reprecipitation from chloroform solution into methanol. After drying, the (co)polymer composition was checked by $^1H$ NMR spectroscopy. No deviations from the comonomer ratio in the feed were found.

**$^1H$ NMR spectra** were recorded on a Bruker AC 250 spectrometer in $CDCl_3$ or mixtures of $CDCl_3$ and trichlorotrifluoroethane (F113) at 20 °C, using the $CHCl_3$ signal (7.26 ppm) and the TMS signal (0 ppm) as internal standards.

**Gel permeation chromatography** was used to determine molecular weights and molecular weight distributions of the synthesized polymers. The system consisted of a Pharmacia P-500 nonpulsating pump coupled with Waters μ-Styragel columns ($10^5$-, $10^4$-, and $10^3$-Å pore sizes) and a 500-Å guard column. Polymer concentration measurements in the eluent were accomplished with a Waters R 403 differential refractometer. Chloroform which was stabilized with up to 1 vol % of ethanol served as eluent at a flow rate of 2 mL/min. The sample concentration was 10 mg/mL; the injection volume was 50 μL for copolymers containing up to 25 mol % of fluorocarbon-substituted repeating units and 150 μL for polymers with a higher fluorine content. The calibration curve was obtained with narrow molecular weight polystyrene standards.

**Thermal analysis** was performed on a Perkin-Elmer DSC-7 equipped with a PE-7700 computer and TAS-7 software. The phase-transition temperatures are given as measured with a heating rate of 10 K/min. Glass transition temperatures as determined by the point of inflection in the heat capacity step were measured with a heating rate of 20 K/min. Gallium and indium were used as the calibration standards.

**Optical polarization microscopy** was done with a Leitz Ortholux II Pol BK microscope equipped with a Mettler FP 82 hot stage.

**Surface tension measurements** were performed on a Krüss K12 torsion balance tensiometer thermostated at 25 °C using a platinum Whilhelmy plate with a perimeter of 59.5 mm.

**Dynamic contact angles** of liquid *n*-alkanes at solid polymer surfaces were determined at 25 °C with the Wilhelmy plate method, using the same tensiometer and Krüss K12c remote control software.

For dynamic measurement of contact angles, the sample plate is immersed and withdrawn from a wetting liquid of known surface tension at a constant speed.[17] The Wilhelmy force, which the meniscus of the wetting liquid exercises on the same plate, is measured in dependence of the immersion depth. Figure 1 shows a typical plot of the overall force acting on the plate versus the immersion depth. The negative slopes are due to the buoyancy force acting on the plate. The average advancing and receding contact angles are calculated by linear regressive extrapolation of the curves obtained for the advancing and receding modes to zero immersion depth. A major advantage of the dynamic method is the reduction of the effect of local surface inhomogenities on the observed contact angles due to the averaging over a large part of the plate surface.[18]

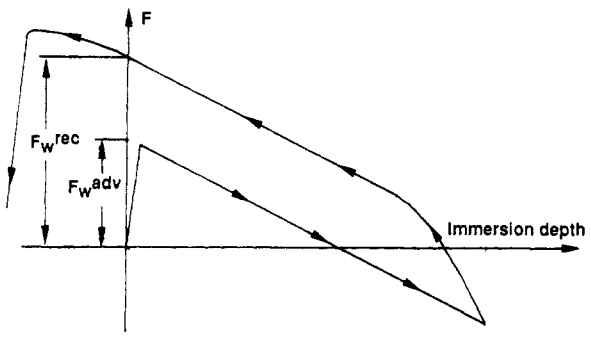


**Figure 1.** Plot of the overall force acting on the sample plate versus the immersion depth as typically obtained with the Wilhelmy plate method. $F_W^{adv}$ and $F_W^{rec}$ denote the extrapolated Wilhelmy forces used for the calculation of the advancing and receding dynamic contact angles, respectively.

Samples for dynamic contact angle measurements were prepared by spin-casting thin films of the fluorocarbon-containing (co)polymers from toluene solution on cover slides for optical microscopy. The casted films were dried for 30 min at 120 °C. *n*-Hexane, *n*-octane, *n*-decane, *n*-dodecane, and *n*-hexadecane used as wetting liquids were of 99% purity. Their surface tensions were determined using the platinum Wilhelmy plate.

## Synthesis

Styrene monomers carrying a fluorocarbon segment were prepared by a phase-transfer-catalyzed etherification of fluorocarbon-substituted alcohols with *p*-(chloromethyl)-styrene.

$$F(CF_2)_n(CH_2)_2OH + ClCH_2C_6H_4CH{=}CH_2 \xrightarrow[\text{NaOH, TBAH [PTC]}]{} F(CF_2)_n(CH_2)_2OCH_2C_6H_4CH{=}CH_2$$

Etherification of fluorinated alcohols using phase-transfer catalysis has already been effectively employed for the synthesis of perfluoroalkyl allyl ethers, using allyl chloride or allyl bromide as the reactant and solvent at the same time.[12,19] However, reaction with an isomeric mixture of para- and meta-substituted (chloromethyl)styrene under the same conditions gave low yields due to partial polymerization of the monomer during synthesis.[20] On the other hand, etherification of alcohols with (chloromethyl)benzene derivatives gave good yields also when equimolar amounts of the reactants and benzene as an inert organic solvent were used.[21]

First we used the latter procedure unaltered for the etherification of fluorocarbon-substituted alcohols. However, when benzene was used as an organic solvent, only low conversions were obtained at a reaction temperature of 40 °C, while carrying out the reaction at 80 °C gave black, viscous oils due to oligomerization of the monomer. In contrast, all reactions were found to proceed to complete conversion when methylene chloride was used as the solvent. $F(CF_2)_4(CH_2)_2OCH_2C_6H_4CH{=}CH_2$ could be purified by vacuum distillation while $F(CF_2)_8(CH_2)_2OCH_2C_6H_4CH{=}CH_2$ was recrystallized several times from methanol. Purification was facilitated by the absence of fluorinated alcohol in the product mixture. Fluorinated reactants were found to be difficult to separate in the synthesis of fluorocarbon-segmented allyl ethers[12] and methacrylates.[13]

Radical polymerization of the fluorocarbon-substituted styrene monomers was carried out with a small amount of solvent added in order to avoid incomplete conversion due to vitrification during polymerization. Homopolymers were prepared as well as copolymers with styrene as the second monomer. Copolymerization parameters have

**Table I**
**Molar Composition, Molecular Weight Characterization, and Surface Data for (Co)polymers Containing Styrene and $F(CF_2)_4(CH_2)_2OCH_2C_6H_4CH{=}CH_2$ Repeating Units[a]**

| copolym composn, mol % $R_F$ | $\gamma_c$, mN/m | $\gamma_s^D$, mN/m | $M_n$ (GPC) | $M_w/M_n$ |
|---|---|---|---|---|
| 100 | 12.0 | 13.0 | | |
| 50 | 17.0 | 15.1 | 11500 | 2.0 |
| 25 | 21.5 | 17.0 | 9300 | 2.2 |
| 10 | 24.0 | 21.5 | 9900 | 2.1 |
| 5 | >25.1 | 23.4 | 9900 | 2.0 |
| 2 | >25.1 | 23.7 | 10300 | 2.1 |

[a] Critical surface tension values ($\gamma_c$) were obtained by extrapolation from data points in the Zisman plot (Figure 5). Dispersion force contributions to the surface energy ($\gamma_s^D$) were extrapolated from the GGFY plot (Figure 7).

**Table II**
**Molar Composition, Molecular Weight Characterization, and Surface Data for (Co)polymers Containing Styrene and $F(CF_2)_8(CH_2)_2OCH_2C_6H_4CH{=}CH_2$ Repeating Units[a]**

| copolym composn, mol % $R_F$ | $\gamma_c$, mN/m | $\gamma_s^D$, mN/m | $M_n$(GPC) | $M_w/M_n$ |
|---|---|---|---|---|
| 100 | 6.0 | 9.0 | | |
| 50 | 10.0 | 11.9 | 12 100 | 2.1 |
| 25 | 13.5 | 13.6 | 13 400 | 2.2 |
| 10 | 17.0 | 17.9 | 12 400 | 2.2 |
| 5 | 18.5 | 18.9 | 11 900 | 1.9 |
| 2 | 21.0 | 22.2 | 13 600 | 2.0 |

[a] Critical surface tension values ($\gamma_c$) were obtained by extrapolation from data points in the Zisman plot (Figure 6). Dispersion force contributions to the surface energy ($\gamma_s^D$) were extrapolated from the GGFY plot (Figure 8).

been reported before by Garnault[20] for the reaction of styrene with an isomeric mixture of para- and meta-substituted $F(CF_2)_6(CH_2)_2OCH_2C_6H_4CH{=}CH_2$ or the corresponding compound containing a sulfur instead of an oxygen bridge. Copolymerizations were found to be almost ideal, and it was concluded that the connection of a long fluorocarbon chain via a hydrocarbon spacer to the aromatic ring has no pronounced effect on the reactivity of the styrene double bond.[20]

The comonomer compositions in the polymers, which we obtained using isomerically pure fluorocarbon-containing comonomers, were determined from the intensity ratios in the $^1H$ NMR spectra and are listed in Tables I and II. As expected, they did not deviate from the composition of the monomer feed.

## Thermal Analysis

The phase behavior of the synthesized monomers and polymers was investigated by differential scanning calorimetry (DSC). While for $F(CF_2)_4(CH_2)_2OCH_2C_6H_4CH{=}CH_2$ only the melting peak was observed, $F(CF_2)_8(CH_2)_2OCH_2C_6H_4CH{=}CH_2$ undergoes a disordering transition at 11 °C before isotropization occurs at 32 °C. In the temperature interval between the two transitions, polarization microscopic observation showed a texture typical for smectic liquid-crystalline phases. This feature was also observed for many other hydrocarbon molecules with long perfluorinated substituents.[9,12,13]

DSC heating traces of the (co)polymers are shown in Figures 2 and 3. The homopolymer from $F(CF_2)_4(CH_2)_2OCH_2C_6H_4CH{=}CH_2$ was completely amorphous, exhibiting a glass transition at 12 °C (Figure 2). $T_g$ values increased with an increase in the fraction of styrene in the copolymers. For the homopolymer from $F(CF_2)_8(CH_2)_2OCH_2C_6H_4CH{=}CH_2$, a melting peak was found at 82 °C in addition to a glass transition at 55 °C (Figure 3). While

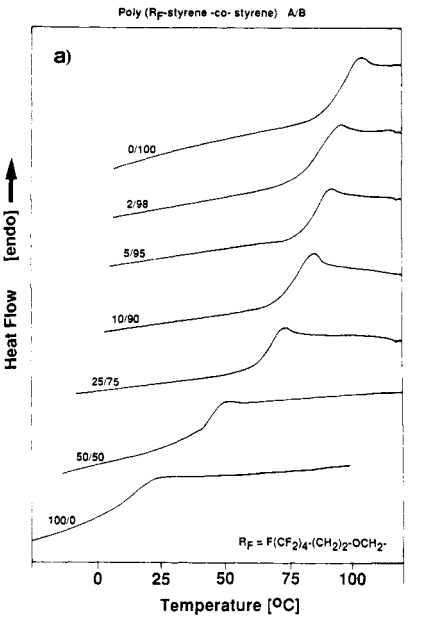


**Figure 2.** DSC heating traces (second heating) of homo- and copolymers containing $F(CF_2)_4$ segments.

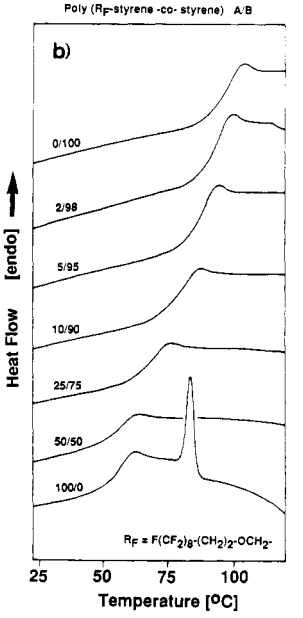


**Figure 3.** DSC heating traces (second heating) of homo- and copolymers containing $F(CF_2)_8$ segments.

the same $T_g$ value was found for the copolymer containing equal molar amounts of perfluorooctyl-substituted styrene and conventional styrene repeating units, no melting peak was observed for this material. Partial crystallinity can be explained by side-chain crystallization of the perfluorooctyl groups. Dilution with nonfunctionalized styrene units prevents packing of the fluorocarbon segments in copolymers with less perfluoroalkyl-substituted styrene content.

A similar behavior has been observed for perfluoroalkyl-substituted polymers with highly flexible backbones, e.g., polysiloxanes[22] and poly(vinyl ethers).[23] While perfluorobutyl and perfluorohexyl substituents gave amorphous polymers, longer fluorocarbon segments caused side-chain crystallization.

Figure 4 summarizes the dependence of $T_g$ values on copolymer composition. Incorporation of low concentrations of [[(perfluorobutylethylene)oxy]methyl]styrene units into the polymer structure leads to a strong decrease

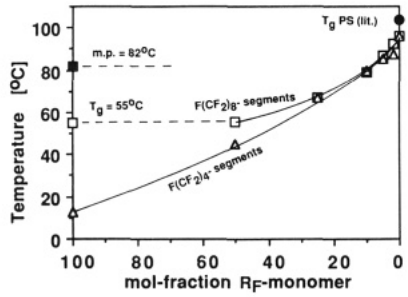


**Figure 4.** Glass transition temperatures plotted versus composition for styrene homo- and copolymers containing $F(CF_2)_4$- or $F(CF_2)_8$-substituted comonomers.

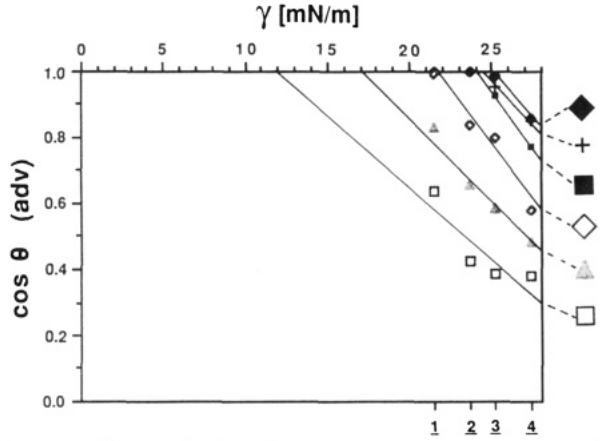


**Figure 5.** Zisman plot for polystyrenes containing various molar fractions of repeating units with $F(CF_2)_4$ segments. Points are values obtained with (1) *n*-octane, $\gamma_L$ = 21.54 mN/m; (2) *n*-decane, $\gamma_L$ = 23.61 mN/m; (3) *n*-dodecane, $\gamma_L$ = 25.14 mN/m; and (4) *n*-hexadecane, $\gamma_L$ = 27.31 mN/m. (◆) $F(CF_2)_4(CH_2)_2OCH_2C_6H_4CH{=}CH_2$ (F4-St) 2 mol %; (+) (F4-St) 5 mol %; (■) (F4-St) 10 mol %; (◇) (F4-St) 25 mol %; (▲) (F4-St) 50 mol %; (□) (F4-St) 100 mol %.

of the $T_g$ compared to pure polystyrene. Copolymers containing perfluorooctyl segments had higher $T_g$'s, which remained constant from 50 to 100% perfluoroalkyl-substituted styrene content, where partial crystallinity was observed.

## Surface Characterization

Critical surface energies of the prepared (co)polymers were determined by *n*-alkane wettability measurements. Films of the polymers were spin-casted onto glass slides and then dried above their glass transition temperature in order to provide sufficient segmental mobility to allow concentration and organization of the fluorinated side chains at the polymer surface. The wettability of the polymer films with a series of *n*-alkanes was then determined by dynamic contact angle measurements. Since these polymers interact with wetting liquids predominantly by dispersion forces, the empirical wetting relation (eq 1) developed by Zisman[4] is a useful way to present wetting data.[24] Plotting the cosine of the contact angle of wetting

$$\cos\theta = 1 + m(\gamma_L - \gamma_c) \quad (1)$$

($\cos\theta$) versus the surface tension of the wetting liquid ($\gamma_L$) yields a straight line with the slope $m$. Extrapolation to the condition of complete wetting of the polymer surface ($\cos\theta = 1$) gives the critical surface tension $\gamma_c$.

Figure 5 shows Zisman plots for homo- and copolymers prepared from styrene and *p*-[[(perfluorobutylethylene)oxy]methyl]styrene. Extrapolated values for the critical surface tension $\gamma_c$ of the materials are summarized in Tables I and II. For the homopolymer, a value of 12 mN/m was found. A similar result was obtained for methacrylate polymers carrying $C_4$ fluorocarbon segments,[24] while the corresponding polysiloxanes had a considerably higher critical surface tension.[25]

As expected, the $\gamma_c$ values for styrene copolymers increased with decreasing fluorocarbon content. For samples with less than 10% fluorocarbon-segmented comonomers, no meaningful extrapolation could be done because a dynamic contact angle could be measured only with *n*-hexadecane and *n*-dodecane, being the ones with highest surface tensions out of the wetting liquids we used. The shorter *n*-alkanes were rapidly adsorbed and spread onto the polymer surface, indicating that their surface tension is lower than the critical surface tension of the solid surface.

In the case of the (co)polymers with perfluorobutyl segments, graphical extrapolation of the data points to $\cos\theta = 1$ could not be done very accurately because of a systematic curvature in the $\cos\theta/\gamma_{solvent}$ dependence for the individual samples. The artificial steepening of the slope is caused by surface solubility effects,[24-26] which become more pronounced with a decrease in the size of the alkane molecules. Solubility leads to an incorporation of wetting liquid into the polymer surface and thus causes an increased surface wettability resulting in higher values for $\cos\theta$.

Surface solubility was also reflected in the large difference between the contact angles measured on immersion ($\theta_{adv}$) and emersion ($\theta_{rec}$) of the samples. Advancing and receding contact angles are given in Table III. Contact angle hysteresis between $\theta_{adv}$ and $\theta_{rec}$ can be caused by various surface imperfections, e.g., roughness, heterogeneity, deformation, and swelling and penetration by the wetting liquid.[17,18]

Doubling the length of the fluorocarbon segment in the side chains of the (co)polymers gave materials which exhibited larger advancing contact angles corresponding to further reduced surface energies. Remarkably, the contact angle hysteresis was below 20° for the homopolymer with perfluorooctyl segments, while hysteresis values above 40° were again obtained for all copolymers. This difference coincides with the observation of side-chain crystallization only for the homopolymer from $F(CF_2)_8(CH_2)_2OCH_2C_6H_4CH{=}CH_2$. The Zisman plot for these (co)polymers is shown in Figure 6. Again, an increase of the $\gamma_c$ values was found with a decrease in the share of fluorocarbon-segmented comonomer in the material composition. However, the absolute values were considerably lower for the materials with perfluorooctyl segments as compared with those of perfluorobutyl-containing samples. Also, artificial steepening of the slopes in the Zisman plot due to surface solubility was reduced considerably.

An extremely low $\gamma_c$ value of 6 mN/m was extrapolated for the homopolymer from *p*-[[(perfluorooctylethylene)oxy]methyl]styrene. As mentioned above, a considerable error margin should be taken into account when extrapolating our wettability data to $\cos\theta = 1$ with the Zisman method. Still, comparably low critical surface tensions have been reported only for monolayers of perfluorocarbon acids or thiols,[4,24] where the fluorocarbon chains are regularly packed in such a way that the $CF_3$ groups form the outermost layer. Formation of ordered layers of fluorocarbon segments in the bulk homopolymer containing perfluorooctyl segments is consistent with the results obtained by DSC indicating crystallization of the side chains.

**Table III**
**Advancing and Receding Contact Angles Measured for (Co)polymers Containing Styrene and $F(CF_2)_8(CH_2)_2OCH_2C_6H_4CH{=}CH_2$ (F8-St) or $F(CF_2)_4(CH_2)_2OCH_2C_6H_4CH{=}CH_2$ (F4-St) Repeating Units**

F8-St

| copolym composn, mol % F8-St | *n*-hexadecane | | *n*-dodecane | | *n*-decane | | *n*-octane | | *n*-hexane | |
|---|---|---|---|---|---|---|---|---|---|---|
| | $\theta_{adv}$, deg | $\theta_{rec}$, deg | $\theta_{adv}$, deg | $\theta_{rec}$, deg | $\theta_{adv}$, deg | $\theta_{rec}$, deg | $\theta_{adv}$, deg | $\theta_{rec}$, deg | $\theta_{adv}$, deg | $\theta_{rec}$, deg |
| 100 | 82 | 68 | 78 | 60 | 71 | 56 | 69 | 47 | 61 | 25 |
| 50 | 71 | 18 | 68 | 21 | 66 | 11 | 59 | 11 | 36 | 12 |
| 25 | 66 | 10 | 63 | 10 | 56 | 11 | 57 | | 18 | 9 |
| 10 | 52 | 9 | 49 | 2 | 47 | | 38 | | 5 | |
| 5 | 49 | 5 | 43 | | 42 | 6 | 34 | | | |
| 2 | 36 | 8 | 30 | 5 | 26 | | 18 | | | |

F4-St

| copolym composn, mol % F4-St | *n*-hexadecane | | *n*-dodecane | | *n*-decane | | *n*-octane | |
|---|---|---|---|---|---|---|---|---|
| | $\theta_{adv}$, deg | $\theta_{re-}$, deg | $\theta_{adv}$, deg | $\theta_{rec}$, deg | $\theta_{adv}$, deg | $\theta_{rec}$, deg | $\theta_{adv}$, deg | $\theta_{rec}$, deg |
| 100 | 68 | 26 | 67 | 17 | 64 | 20 | 58 | 13 |
| 50 | 61 | 21 | 54 | 10 | 46 | 5 | 34 | 10 |
| 25 | 50 | 15 | 38 | 10 | 40 | 5 | 6 | 5 |
| 10 | 39 | 6 | 22 | 2 | 4 | | | |
| 5 | 31 | | 18 | 1 | | | | |
| 2 | 23 | | 9 | | | | | |

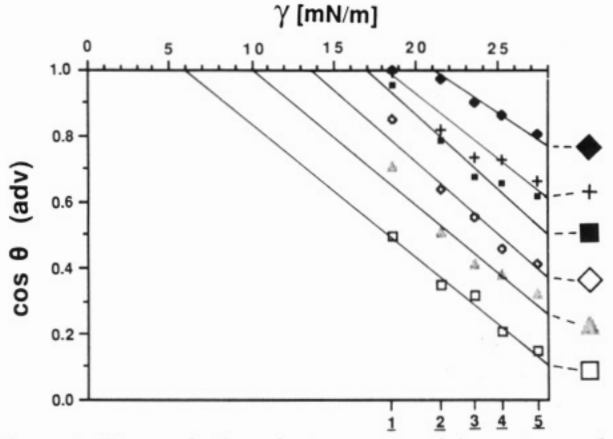


**Figure 6.** Zisman plot for polystyrenes containing various molar fractions of repeating units with $F(CF_2)_8$ segments. Points are values obtained with (1) *n*-hexane, $\gamma_L$ = 18.58 mN/m; (2) *n*-octane, $\gamma_L$ = 21.54 mN/m; (3) *n*-decane, $\gamma_L$ = 23.61 mN/m; (4) *n*-dodecane, $\gamma_L$ = 25.14 mN/m; and (5) *n*-hexadecane, $\gamma_L$ = 27.31 mN/m. (◆) $F(CF_2)_8(CH_2)_2OCH_2C_6H_4CH{=}CH_2$ (F8-St) 2 mol %; (+) (F8-St) 5 mol %; (■) (F8-St) 10 mol %; (◇) (F8-St) 25 mol %; (▲) (F8-St) 50 mol %; (□) (F8-St) 100 mol %.

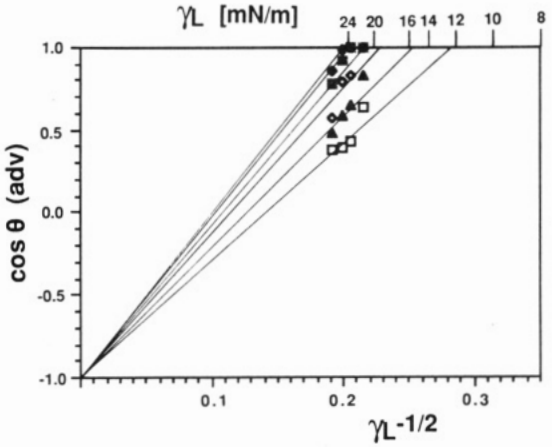


**Figure 7.** Girifalco–Good–Fowkes–Young plot for polystyrenes containing various molar fractions of repeating units with $F(CF_2)_4$ segments. Points are values obtained with (◆) $F(CF_2)_4$-$(CH_2)_2OCH_2C_6H_4CH{=}CH_2$ (F4-St) 2 mol %; (+) (F4-St) 5 mol %; (▣) (F4-St) 10 mol %; (◇) (F4-St) 25 mol %; (▲) (F4-St) 50 mol %; (□) (F4-St) 100 mol %.

The *n*-alkane wettability data were also used to determine the dispersion force component of the surface energy, $\gamma_s^D$, according to the Girifalco–Good–Fowkes–Young equation[27,28] (eq 2) as used by other authors.[25,26] In a plot

$$\cos\theta = -1 + 2(\gamma_s^D)^{1/2}\,\gamma_L^{-1/2} \qquad (2)$$

$\gamma_s^D$ = dispersive surface energy of solid

$\gamma_L$ = surface tension of wetting liquid

of cos $\theta$ versus $\gamma_L^{-1/2}$, the experimental data for cos $\theta$ obtained for various *n*-alkanes as wetting liquids should give a straight line intercepting the cos $\theta$ axis at −1 and the horizontal line at cos $\theta$ = +1 at $(\gamma_s^D)^{1/2}$.

Figures 7 and 8 show such Girifalco–Good–Fowkes–Young (GGFY) plots for the dynamic advancing contact angle data obtained for the series of styrene (co)polymers containing $F(CF_2)_4(CH_2)_2OCH_2C_6H_4CH{=}CH_2$ and $F(CF_2)_8(CH_2)_2OCH_2C_6H_4CH{=}CH_2$ repeating units, respectively. Extrapolated values for the dispersive surface energy $\gamma_s^D$ of the materials are summarized in Tables I and II.

The error margins of the extrapolation of the data points were considerably reduced compared to the evaluation of the Zisman plots, because all straight lines start from the same origin at $\theta$ = 180° when $\gamma_s^D$ = 0. Comparison of the data in Table I shows that $\gamma_s^D$ values for copolymers containing $F(CF_2)_4$ segments are about 2 mN/m lower than the $\gamma_c$ values obtained from the Zisman plot (Figure 5). This difference might be explained partly by the inaccuracy of the extrapolation in the Zisman plot. However, the persistence of the deviation over a large range of copolymer compositions suggests a real difference in the apparent dispersive surface energy and the critical surface tension. This might indicate that the polymer/solvent interaction is not purely dispersive, as was first postulated for other glassy fluorocarbons by Fowkes.[29]

For copolymers containing up to 50 mol % of $F(CF_2)_8$-substituted comonomer, the extrapolated values for critical surface tensions and dispersive surface energies agree very well. In the case of the homopolymer from $F(CF_2)_8$-$(CH_2)_2OCH_2C_6H_4CH{=}CH_2$ and the corresponding copolymer containing 50 mol % of styrene units, the dispersive surface energy is higher than the critical surface tension. Considering the comparative fluoropolymer surface tension data compiled recently by Kobayashi and Owen,[26] this tendency seems to be generally observed for

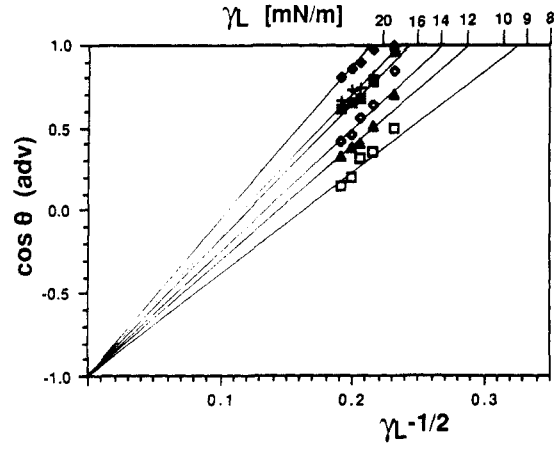


**Figure 8.** Girifalco–Good–Fowkes–Young plot for polystyrenes containing various molar fractions of repeating units with $F(CF_2)_8$ segments. Points are values obtained with (◆) $F(CF_2)_8$-$(CH_2)_2OCH_2C_6H_4CH{=}CH_2$ (F8-St) 2 mol %; (+) (F8-St) 5 mol %; (■) (F8-St) 10 mol %; (◇) (F8-St) 25 mol %; (▲) (F8-St) 50 mol %; (□) (F8-St) 100 mol %.

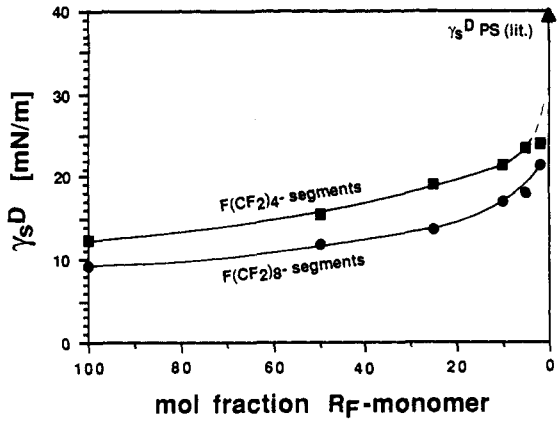


**Figure 9.** Plot of the dispersion force contribution to the surface energy $\gamma_s^D$ versus the molar composition of (co)polymers.

polymers with long fluorocarbon substituents. No explanation can be given yet.[26]

For the homopolymer from p-[[(perfluorooctylethylene)oxy]methyl]styrene, the dispersion force component of the surface energy was 9.3 mN/m. Again, this value is similar to those obtained for monolayers of perfluorocarbon acids,[30] which exhibit the lowest known dispersive surface energies. Thus, both $\gamma_c$ and $\gamma_s^D$ values indicate a rather ordered packing of the perfluorooctyl segments exposing the $CF_3$ groups at the surface of the material.

In Figure 9, the dispersion force component of the surface energy of the (co)polymers is plotted versus the mole fraction of perfluoroalkyl-substituted repeating units. A slow, roughly linear increase of $\gamma_s^D$ is observed for both sets of copolymers as the concentration of the fluorinated units is reduced from 100 to 10%. In absolute values, the dispersive surface energies found for the perfluorooctyl-substituted polymer series were about 4 mN/m lower than those extrapolated for the perfluorobutyl-containing series. For mole fractions below 10%, a steepening of the $\gamma_c$ increase can be seen. Values for copolymers containing 5 and 2% of perfluorobutyl-segmented comonomer have been omitted because for these samples a contact angle could only be obtained with *n*-hexadecane as the wetting liquid, while *n*-dodecane was adsorbed and spread on the polymer surface.

It is remarkable, however, that copolymers with only 5 and 2 mol % perfluorooctyl-substituted comonomer showed surface energy characteristics comparable to those of poly(tetrafluoroethylene) and poly(dimethylsiloxane),[26] respectively. Such behavior points to a pronounced surface activity of the fluorocarbon-substituted repeating units in polystyrene surroundings.

## Conclusions

Results obtained for styrene-based polymers which contain perfluorocarbon-segmented side chains indicate that the surface characteristics of the materials depend on the organizational state of the fluorocarbon segments. Low surface energies demonstrate that highly ordered fluorocarbon surfaces can be formed due to crystallization of the side chains. This was universally observed for different polymers containing fluorocarbon segments with at least eight carbon atoms. In the case of flexible polymer backbones (polysiloxanes[21] and poly(vinyl ethers)[23]), crystallization occurred at lower temperatures than those for more rigid ones (polymethacrylates[31] and polystyrenes). At a temperature below the melting of the side chains, an extremely low surface energy was observed for poly[*p*-[[(perfluorooctylethylene)oxy]methyl]styrene]. Similar surface data have only been obtained for monolayers of perfluorocarbon acids on solid substrates.[30] In contrast, higher surface tension values which have been reported in the literature for polysiloxanes with long fluorocarbon segments[25,26] have all been measured at temperatures above the melting of the side chains.

For the corresponding polystyrene with perfluorobutyl segments no side-chain crystallization was observed, and the surface data measured for this material are comparable to those reported for many other polymers with short fluorocarbon substituents.[26]

Incorporation of unsubstituted styrene units in the polymer backbone resulted in a gradual increase of the surface energy, which became more steep as the styrene fraction exceeded 50%. In the case of large styrene fractions, a disordered surface may be expected. No side-chain crystallization was observed for the corresponding polymers. In the case of smaller styrene fractions, comonomer fraction dependent variations of the surface energy might be due to formation of structural defects and domain boundaries resulting from an island structure.

Compared to a surface of pure polystyrene, a drastic lowering of the surface energy was observed when a few percent of fluorocarbon-containing comonomer units was incorporated into the polymer structure. This indicates preferential adsorption of the fluorocarbon segments at the surface of the material, which is caused by the incompatibility of fluorocarbon moieties with the bulk hydrocarbon matrix. With an increase in the length of the perfluorinated segment, a smaller fraction yielded a more pronounced decrease of the surface energy. This correlation has also been observed for solutions of surface-active low molecular weight fluorocarbon–hydrocarbon molecules in organic solution, where the addition of 0.1 mol % of the molecules with a perfluorododecyl moiety caused a drastic decrease of the surface tension.[12,13] Thus, the incorporation of fluorocarbon segments longer than perfluorooctyl should result in reduction of the minimal amount necessary to achieve a considerable effect on the surface energy of the polymer, and at the same time it should also reduce the threshold concentration needed for the formation of an ordered layer of fluorocarbon segments resulting in extremely low surface tension values.

In conclusion, surface activity and self-organization of fluorocarbon–hydrocarbon compounds can be exploited for the modification of polymeric materials with an inherent protective coating and low friction surfaces.

**Acknowledgment.** We thank Dr. K. v. Werner and Dr. G. Siegemund, Hoechst AG, for providing valuable fluorinated compounds. We are grateful to Nagase & Co. Ltd., Tokyo, Japan, for a gift of *p*-(chloromethyl)styrene. We thank the technical team of Krüss GmbH, Hamburg, FRG, for allowing us to test development versions of their CAMS contact angle measuring software and for many helpful discussions.

## References and Notes

(1) England, D. C.; Uschhold, R. E.; Starkweather, H.; Pariser, R. *Proc. Robert A. Welch Found. Conf. Chem. Res.* **1982**, *26*, 193–243.
(2) Meussdoerffer, J. N.; Niederprüm, H. *Chem. Zeit.* **1980**, *104*, 45.
(3) Collins, S. H. *Plast. Compd.* **1983**, *6*, 38.
(4) Zisman, W. A. *Contact Angle, Wettability, and Adhesion*; Advances in Chemistry Series 43; American Chemical Society: Washington, DC, 1964.
(5) Chidsey, C. E. D.; Loiacono, D. N. *Langmuir* **1990**, *6*, 682.
(6) Schneider, J.; Erdelen, C.; Ringsdorf, H.; Rabolt, J. F. *Macromolecules* **1989**, *22*, 3475.
(7) Torstensson, M.; Ranby, B.; Hult, A. *Macromolecules* **1990**, *23*, 126.
(8) Higashi, N.; Kunitake, T. *Chem. Lett.* **1986**, 105.
(9) Höpken, J.; Pugh, C.; Richtering, W.; Möller, M. *Makromol. Chem.* **1988**, *189*, 911.
(10) Rabolt, J. F.; Russell, T. P.; Twieg, R. J. *Macromolecules* **1984**, *17*, 2786.
(11) Russell, T. P.; Rabolt, J. F.; Twieg, R. J.; Siemens, R. L.; Farmer, B. L. *Macromolecules* **1986**, *19*, 1135.
(12) Höpken, J.; Möller, M.; Boileau, S. *New Polym. Mater.* **1991**, *2*, 339.
(13) Höpken, J.; Faulstich, S.; Möller, M., submitted for publication in *Mol. Cryst. Liq. Cryst.*
(14) Mahler, W.; Guillon, D.; Skoulios, A. *Mol. Cryst. Liq. Cryst., Lett. Ed.* **1985**, *2*, 111.
(15) Viney, C.; Russell, T. P.; Depero, L. E.; Twieg, R. J. *Mol. Cryst. Liq. Cryst.* **1989**, *168*, 63.
(16) Turberg, M. P.; Brady, J. E. *J. Am. Chem. Soc.* **1988**, *110*, 7797.
(17) Andrade, J. D.; Smith, L. M.; Gregoris, D. E. In *Surface and Interfacial Aspects of Biomedical Polymers*; Andrade, J. D., Ed.; Plenum Press: New York, 1985.
(18) Johnson, R. E., Jr.; Dettre, R. H. Wettability and Contact Angles. In *Surface and Colloid Science*; Matijevic, E., Ed.; Wiley-Interscience: New York, 1969; Vol. 2, p 85.
(19) Boutevin, B.; Youssef, B.; Boileau, S.; Garnault, A. M. *J. Flourine Chem.* **1987**, *35*, 399.
(20) Garnault, A. M. Thèse de Docteur Ingénieur, Université Pierre et Marie Curie, Paris, 1986.
(21) Percec, V.; Kennedy, J. P. *Polym. Bull.* **1983**, *10*, 31.
(22) Dorigo, R. Thèse de Docteur Ingénieur, Université Pierre et Marie Curie, Paris, 1989.
(23) Höpken, J.; Möller, M.; Lee, M.; Percec, V., submitted for publication in *Makromol. Chem.*
(24) Johnson, R. E., Jr.; Dettre, R. H. *Polym. Prepr. (Am. Chem. Soc., Div. Polym. Chem.)* **1987**, *28*, 48.
(25) Doeff, M. M.; Lindner, E. *Macromolecules* **1989**, *22*, 2951.
(26) Kobayashi, H.; Owen, M. J. *Macromolecules* **1990**, *23*, 4929.
(27) Fowkes, F. M. *J. Phys. Chem.* **1962**, *66*, 382.
(28) Girifalco, L. A.; Good, R. J. *J. Phys. Chem.* **1957**, *61*, 904.
(29) Fowkes, F. M.; Sawyer, W. M. *J. Chem. Phys.* **1952**, *20*, 1650.
(30) Dann, J. R. *J. Colloid Interface Sci.* **1970**, *32*, 302.
(31) Höpken, J.; Möller, M., in preparation.